Brownian Motion of a Rough Sphere and the Stokes−Einstein Law†

J. R. Schmidt and J. L. Skinner*

Theoretical Chemistry Institute and Department of Chemistry, University of Wisconsin, Madison, Wisconsin 53706

Received: October 21, 2003; In Final Form: January 14, 2004

Using molecular dynamics computer simulation, we have calculated the velocity autocorrelation function and diffusion constant for a variety of solutes in a dense fluid of spherical solvent particles. We explore the effects of surface roughness of the solute on the resulting hydrodynamic boundary condition as we naturally approach the Brownian limit (when the solute becomes much larger and more massive than the solvent particles). We find that when the solute and solvent interact through a purely repulsive isotropic potential, in the Brownian limit the Stokes−Einstein law is satisfied with slip boundary conditions. However, when surface roughness is introduced through an anisotropic solute−solvent interaction potential, we find that the Stokes−Einstein law is satisfied with stick boundary conditions. In addition, when the attractive strength of a short-range isotropic solute−solvent potential is increased, the solute becomes dressed with solvent particles, making it effectively rough, and so stick boundary conditions are again recovered.

I. Introduction

The diffusive motion of a large solute particle in a fluid of much smaller solvent particles is a problem with great historical roots, and of much practical importance.[1−3] Treating the fluid as a hydrodynamic continuum, the diffusion constant, D, of such a solute is given by the Stokes−Einstein equation,

$$D = \frac{kT}{c\pi\eta R} \tag{1}$$

where T is the absolute temperature, R is the radius of the (spherical) solute, η is the shear viscosity of the neat solvent, and c is a constant determined by the choice of hydrodynamic boundary conditions applied at the surface of the sphere, which is 4 or 6 for slip or stick conditions, respectively. The slip boundary condition assumes that the normal component of fluid velocity at the fluid−solute interface is zero and that the fluid exerts no stress along the solute's surface, whereas the stick boundary condition demands zero relative fluid−solute velocity (both normal and tangential) at the interface.

In a recent paper[4] we showed by computer simulation that for a solute interacting with solvent particles with a weakly attractive isotropic potential, the Stokes−Einstein equation holds with slip boundary conditions as the size and mass of the solute become large with respect to the solvent particles, and similar results have also been found by others.[5] However, experimentally, it is found for a mesoscopic solute that stick boundary conditions apply.[6,7] This raises the question as to the molecular origins of the stick boundary condition.

One intuitive hypothesis is that the stick boundary condition arises due to the inevitable roughness that characterizes any mesoscopic surface on a molecular level. Richardson demonstrates, for a particular periodic roughness of a flat surface, how the stick boundary condition naturally arises on a macroscopic level regardless of whether stick *or* slip boundary conditions are applied microscopically at the surface.[8] Several molecular dynamics (MD) simulations also seem to suggest a connection between surface roughness and stick boundary conditions. Both Khare et al.[9] and Koplik et al.[10] use nonequilibrium MD methods to show that the stick boundary condition applies in Couette flow between two atomistic fcc lattice walls. An MD simulation by Bocquet and Barrat demonstrates a transition between slip and stick boundary conditions as corrugation is introduced onto the walls.[11] Similarly, Thompson and Robbins show a transition from stick to slip as the packing density of the atoms in the walls increases (and thus the walls become molecularly smooth).[12]

There are only a few examples of MD simulations of a rough solute particle in the Brownian limit. Vergeles et al. used nonequilibrium MD methods to measure the force on a solute moving at a constant velocity through a bath of smaller particles.[13] They obtain results consistent with stick boundary conditions for *both* rough and smooth solutes, in contrast to other results for smooth solutes.[4,5] However, using equilibrium methods for the smooth solute, they obtain results consistent with slip boundary conditions. Heyes et al.[14] also carried out an MD simulation of a large rough colloid particle with atomistic detail. They also concluded that the Stokes−Einstein equation held with stick boundary conditions. However, in a similar calculation for a smooth colloid particle Heyes et al. also find stick boundary conditions to hold. We suspect that this result may be due to a neglect of the contribution to the diffusion coefficient from the well-known long-time tail.

Theoretical calculations also shed some light on the origins of the stick boundary condition.[15−23] In a mode-coupling type calculation, Masters and Madden show that for a steeply repulsive radial potential, slip boundary conditions are obtained.[15] However, for a certain choice of parameters such that the force between the Brownian and fluid particles is proportional to their relative velocity, stick boundary conditions are (almost) recovered. Bagchi and co-workers, using both mode-coupling theory[16] and MD simulation,[17] demonstrated a transition between "subslip" and "superstick" boundary conditions as the strength of the solute−solvent interaction is increased. However, these studies did not involve the Brownian limit, as

† Part of the special issue "Hans C. Andersen Festschrift".

10.1021/jp037185r CCC: $27.50
Published on Web 03/09/2004

the solute and solvent particles were the same size. Various other theoretical approaches have demonstrated that diffuse reflections (perhaps caused by surface roughness) lead to stick boundary conditions, whereas specular reflections lead to slip.[24,25]

To examine the origins of the stick boundary condition as it applies to Brownian motion, and more generally to understand the effect of the solute−solvent potential on the solute's diffusion constant, we have carried out a series of MD simulations involving several different model systems. The first model involves a purely repulsive isotropic solute−solvent potential. In our previous work we considered a weakly attractive isotropic solute−solvent potential.[4] Our expectation is that in the Brownian limit the presence or absence of a weak attraction should not be important, but we wanted to verify this explicitly. We find, in fact, that, like the weakly attractive case, slip boundary conditions are more or less satisfied, as long as the solute radius is taken to be the effective hydrodynamic radius. The second model involves a rough solute particle, which is represented as a rigid cluster of solvent particles, each of which interact with the true solvent particles with the solvent−solvent (Lennard-Jones) potential. We find that for this model, as long as the effective hydrodynamic radius is used for the rough solute, stick boundary conditions apply. Finally, the third model is designed to illustrate some aspects of the crossover from slip to stick boundary conditions. Here we consider a short-range isotropic solute−solvent interaction with variable attraction. For weak attraction we expect to find slip boundary conditions (and we do), as in the above examples. However, when the attraction becomes sufficiently strong, the solute becomes "dressed" or "decorated" with a strongly bound solvation shell, rendering it effectively rough, in which case stick boundary conditions are found to apply.

II. Repulsive Isotropic Solute−Solvent Potential

In a previous paper[4] we found that slip boundary conditions hold when a large, massive solute interacts with the surrounding solvent particles with a simple, weakly attractive isotropic potential. To examine the effect of the attractive part of the potential on the hydrodynamic boundary condition, we will reexamine this model problem using a modified interaction potential in which the attractive part has been removed. As before, the solvent−solvent interactions are described in a pairwise additive fashion by a simple Lennard-Jones (LJ) potential,

$$\phi(r) = 4\epsilon[(\sigma/r)^{12} - (\sigma/r)^{6}] \tag{2}$$

which was truncated at 2.5 σ, whereas solute−solvent interactions are given by the following modified Weeks−Chandler−Anderson (WCA) potential,[26]

$$\psi(r) = 4\epsilon\left[\left(\frac{\sigma}{r-a}\right)^{12} - \left(\frac{\sigma}{r-a}\right)^{6}\right] + \epsilon \tag{3}$$

for $0 \le (r - a)/\sigma \le 2^{1/6}$, and zero otherwise. This potential is simply obtained from our previous modified LJ potential[4,27,28] by truncating at the minimum and shifting. Thus this solute−solvent pair potential has the same form as a conventional WCA potential but is simply shifted out in distance by an amount a to account for the larger solute size.

Because the solvent particles interact via an attractive potential, it seems natural to define the solvent radius as half the distance at which $\phi(r)$ is zero. This then implies that the solvent radius is $\sigma/2$. However, we cannot use this procedure in defining the solute radius because the solute−solvent interaction is purely repulsive. In this case, it seems reasonable to define the sum of solvent and solute radii as the separation such that the interparticle repulsion is kT. Given that we are interested in the liquid region of the LJ phase diagram, where $kT \approx \epsilon$, and because $\psi(a + \sigma) = \epsilon$, we therefore define the sum of the solvent and solute radii to be $a + \sigma$, and so the solute radius is $a + \sigma/2$.

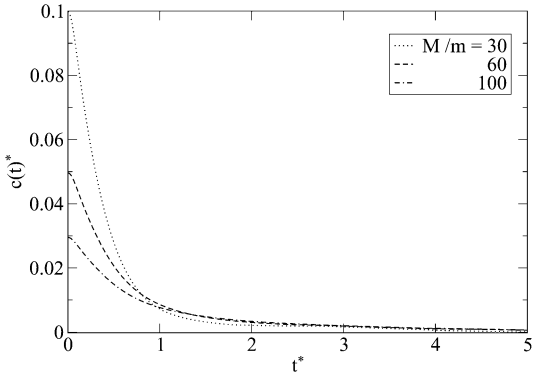

Figure 1. Solute VACFs, for the case of purely repulsive isotropic solute−solvent interactions, for a variety of solute−solvent mass ratios.

In studying solutes of different sizes, it is most appropriate to let the mass of the solute vary with the size, so as to keep the solute's mass density constant. In fact, for simplicity we set the mass densities of the solute and solvent particles to be equal.[4] Using this condition, we define

$$a = (\sigma/2)[(M/m)^{1/3} - 1] \tag{4}$$

where M and m are the solute and solvent masses, respectively. Thus, in this way the solute may be varied in a physically meaningful manner as the Brownian limit ($M/m \rightarrow \infty$, and so $a \rightarrow \infty$) is approached.

We performed simulations of a single solute in a solution of 8787 solvent particles at a reduced solvent density ($\rho^* = \rho\sigma^3$) of 0.85 and at a reduced temperature ($T^* = kT/\epsilon$) of 1.0. The reduced time step ($\delta t^* = \delta t(\epsilon/m\sigma^2)^{1/2}$) was set to 0.005, and the equations of motion were integrated using the Verlet-leapfrog method.[29] A complete description of the MD simulations details is given elsewhere.[4]

The solute velocity autocorrelation functions (VACFs),

$$c(t) = \langle \vec{v}(t) \cdot \vec{v}(0) \rangle \tag{5}$$

for several representative solute−solvent mass ratios are shown in Figure 1 (here $c(t)^* = c(t)m/\epsilon$). The solute diffusion constants are calculated from the VACF using the Green−Kubo expression

$$D = \frac{1}{3}\int_0^\infty c(t)\, \mathrm{d}t \tag{6}$$

We accounted for contributions beyond the maximum simulation time by fitting the VACF at long time to the expected $t^{-3/2}$ asymptotic form and adding the appropriate correction as described elsewhere.[4] The resulting diffusion constants are presented in Table 1 (here $D^* = D(m/\epsilon\sigma^2)^{1/2}$). The hydrodynamic boundary condition coefficient c can now be calculated (see eq 1) from

$$c = \frac{kT}{D\pi\eta R} \tag{7}$$

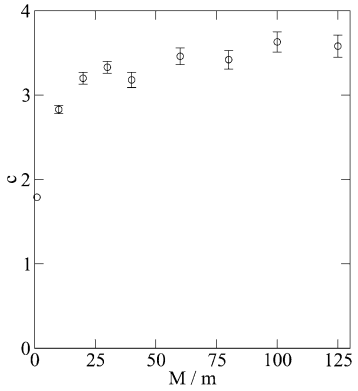

Figure 2. Hydrodynamic boundary condition coefficient values, for the case of purely repulsive isotropic solute−solvent interactions, for a variety of solute−solvent mass ratios.

TABLE 1: Diffusion Constants, for the Case of Purely Repulsive Isotropic Solute−Solvent Interactions, for a Variety of Solute−Solvent Mass Ratios

M/*m*	*D**
1	0.0631 ± 0.00098
10	0.0252 ± 0.00042
20	0.0190 ± 0.00040
30	0.0165 ± 0.00037
40	0.0161 ± 0.00044
60	0.0133 ± 0.00037
80	0.0124 ± 0.00040
100	0.0110 ± 0.00036
125	0.0105 ± 0.00037

The viscosity, η, was previously calculated for the neat solvent, with the result that $\eta^* = \eta\sigma^2/(m\epsilon)^{1/2} = 2.83 \pm 0.06$.[4]

Following the example of our previous work[4] the effective hydrodynamic radius, *R*, at which the hydrodynamic boundary conditions are applied, was set to $r' + r = \sigma + a$, where r' and r are the solute and solvent radii, respectively. This result can be justified intuitively by noting that $r' + r$ is also essentially the distance of closest approach between solute and solvent particles, and indeed, it would seem strange to apply the hydrodynamic boundary conditions at a distance smaller than this.

c is calculated for each mass ratio using eq 7, and the results are shown in Figure 2. The hydrodynamic boundary condition coefficient increases from $c = 1.8$ for $M/m = 1$, to $c = 3.6$ when $M/m = 125$. Finite-size effects prevent the exploration of larger solute−solvent mass ratios. The figure suggests that *c* is still slowly increasing with solute mass, but the results seem consistent with an asymptotic approach to $c = 4$, corresponding to slip boundary conditions.

The eventual convergence of *c* to the slip value is really not surprising. A precise statement of the slip boundary condition is that there there is no tangential stress, i.e., no torque, on the solute, and that the requisite normal boundary condition imposed by the impenetrability of the solute to solvent applies as well. Even though these boundary conditions do not apply on a microscopic scale, they would be expected to be appropriate as the solute size increases. Because the solute−solvent potential is isotropic, and thus the solvent can exert no torque on the solute, the slip boundary condition seems to be a much more reasonable choice than the stick condition, which demands equality of the tangential velocities.

We can compare these results with those previously obtained for our weakly attractive modified LJ potential.[4] In the present case the approach to the asymptotic value seems slower when compared to the attractive potential, where the boundary condition coefficient had almost reached its asymptotic value by $M/m = 100$. This may simply be a reflection of the fact that the current model starts farther from the asymptotic limit (with $c = 1.8$ for $M/m = 1$) than did the previous one (with $c = 2.25$ for $M/m = 1$). However, it may also reflect the uncertainty in the definition of the hydrodynamic radius of the purely repulsive solute. Although this uncertainty becomes negligible as the solute increases to mesoscopic size, it does affect the rate at which the hydrodynamic boundary condition approaches its asymptotic value as a function of solute size.

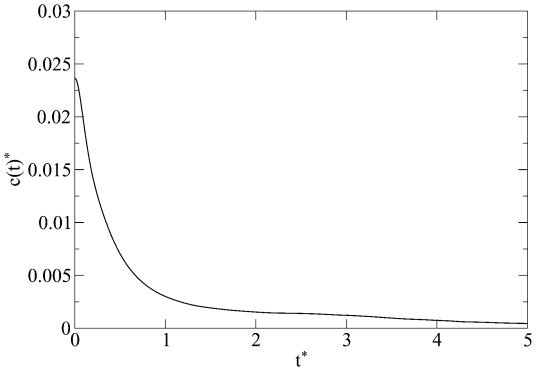

Figure 3. VACF for the rough solute.

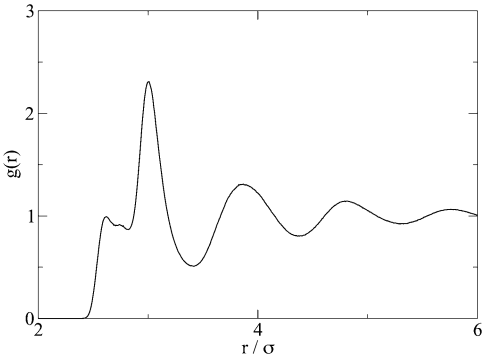

Figure 4. Solute−solvent radial distribution function for the rough solute.

III. Rough Solute

Unlike a smooth solute, a rough solute can interact with the surrounding solvent in such a way that a net torque is exerted. Such a torque could provide a molecular mechanism for enforcing the constraints imposed by stick boundary conditions. To examine the effects of surface roughness of the Brownian solute on the hydrodynamic boundary condition, we carried out an MD simulation of a large rough particle. The solvent particles were modeled with simple LJ interactions, as described above, and the solute was modeled by a rigid cluster of 73 LJ particles. Twelve particles were placed symmetrically around a central particle at a distance of σ, and the remaining 60 of the LJ particles were placed at the vertexes of a truncated icosahedron (a "buckeyball") at a distance of 2σ from the center. All (solute and solvent) LJ interactions are given by eq 2. The mass of each LJ particle in the solute was scaled by a factor of 1.71, resulting in a solute with a mass of 125*m*, and of approximately the same mass density as the solvent particles.

The solute was treated as a rigid body, and an MD simulation was carried out as described above (except now with rigid-body solute rotations). The VACF and solute−solvent radial distribution functions are shown in Figures 3 and 4, respectively. The translational diffusion constant for the solute was calculated by integrating the VACF. A correction was applied to account for

TABLE 2: Diffusion Constants, for the Case of Short-Range Isotropic Variably Attractive Solute−Solvent Interactions, as a Function of ϵ_s/ϵ

ϵ_s/ϵ	D^*
1	0.0101 ± 0.00037
2	0.00824 ± 0.00029
3	0.00699 ± 0.00025
5	0.00539 ± 0.00021
7	0.00494 ± 0.00020
9	0.00459 ± 0.00019
11	0.00446 ± 0.00019

the long-time tail, as previously described. The resulting diffusion constant was found to be $D^* = 0.00634 \pm 0.00026$.

Because the solvent and solute interact with an attractive potential, we define the solute radius by when the solute−solvent potential is zero, as we did in our previous paper.[4] In particular, we focus on the case when the solvent particle is approaching in a radial direction collinear with an outer solute LJ particle. Using this definition, we find that the solute radius is essentially (because the solute's inner LJ particles contribute only a very small amount to the solute−solvent potential at physical distances) $5\sigma/2$, and so the hydrodynamic radius is 3σ. Figure 4 shows that, due to the gaps between the solute's outer-shell LJ particles, some solvent particles can actually approach somewhat closer than the hydrodynamic radius. We believe that this "inner radius", defined for example by the point at which the radial distribution function falls nearly to zero, does not lead to a reasonable definition of the hydrodynamic radius. For example, a solvent particle moving around the surface of the solute at a distance of this inner radius would encounter very large potential barriers, whereas the same particle moving at the hydrodynamic radius would encounter barriers on the order of kT.

The hydrodynamic boundary condition coefficient was calculated using using eq 7 with $R = 3\sigma$, yielding $c = 5.92 \pm 0.24$, consistent with stick boundary conditions. In contrast, the results obtained for a smooth solute of the same mass and size, with either purely repulsive or attractive[4] interactions, were $c = 3.58$ or 3.98, respectively, indicative of slip boundary conditions. The contrast between these results suggest that the addition of the surface roughness, which fundamentally alters the interactions between the solute and solvent, results in a transition from slip to stick boundary conditions.

IV. Strongly Attractive Isotropic Solute−Solvent Potential

As a final model problem, to investigate some aspects of the crossover from slip to stick boundary conditions, we suppose that the solute−solvent potential is short-range and isotropic, but with a variable attraction. When the attraction is weak, similar to the case studied previously,[4] slip boundary conditions should be appropriate. But as the attraction increases, the first solvation shell of the solute becomes nearly permanently affixed near the surface of the solute (at the potential minimum), thus creating an effectively rough sphere composed of a large smooth core and a rough surface.

We are motivated by previous MD results for planar flow between two rough walls. Koplik et al. show that as the interaction strength between the walls and fluid increase, the location at which the stick boundary condition applies moves deeper into the fluid, as if the first layer of solvent had become part of the wall.[10] Similar results were obtained by Bagchi and co-workers, who calculated the change in the diffusion constant of (or using MCT techniques, the friction on) a solute particle as the strength of specific solute−solvent interactions was increased.[16,17] Note that in these studies the solute and solvent particles were both of diameter σ. They found that, in the limit of strong solute−solvent interactions, the diffusion constant decreased (and the friction increased) by a factor 3. They explained this result by assuming that the first solvation shell adhered to the solute, and thus formed a "solvent-berg" of diameter 3σ.

We consider an attractive isotropic solute−solvent potential of the form

$$\psi(r) = 4\epsilon_s\left[\left(\frac{\sigma}{r-a}\right)^{12} - \left(\frac{\sigma}{r-a}\right)^{6}\right]S(r-a) \qquad (8)$$

where the switching function $S(r)$[30] is 1 for $r < r_1$,

$$S(r) = (r_2^2 - r^2)^2(r_2^2 + 2r^2 - 3r_1^2)/(r_2^2 - r_1^2)^3 \qquad (9)$$

for $r_1 < r < r_2$, and zero for $r > r_2$. We take $r_1 = 2^{1/6}\sigma$, $r_2 = 3\sigma/2$. Thus this is a shifted (in the radial direction) LJ potential with an adjustable well depth ϵ_s, multiplied by a switching function that starts turning off at the potential minimum and goes to zero by $r = a + 3\sigma/2$. This potential is designed so that it has a strong but short-range attraction. As the well depth is increased, solvent particles (but only in the first solvation shell) become strongly bound to the solute. In this limit, similar behavior to a conventional rough solute would be expected.

An MD simulation was carried out for a variety of solute−solvent interaction strength ratios ϵ_s/ϵ, with $M/m = 100$, and in each case the resulting VACF was used to calculate the solute diffusion constant, as described above; the results are shown in Table 2.

To determine the hydrodynamic boundary condition coefficient, one needs to define the hydrodynamic radius. When the attraction is weak ($\epsilon_s = \epsilon$), the hydrodynamic radius should presumably be $a + \sigma$, as before. Using this choice, we obtain $c = 3.98 \pm 0.15$, indicative of slip boundary conditions as we would expect. On the other hand, for large enough ϵ_s/ϵ, we anticipate that the hydrodynamic radius should be that appropriate for the solute and its first solvation shell. The particles in the first solvation shell sit directly at the potential minimum of the solute−solvent interaction, which is at $a + 2^{1/6}\sigma$. Similar to before, the hydrodynamic radius of the composite cluster was then determined by when the solute−solvent potential is zero, for a solvent particle approaching in a radial direction collinear with an outer composite cluster atom. Using this criteria, we find

$$R = a + (1 + 2^{1/6})\sigma \qquad (10)$$

With this choice for the hydrodynamic radius, c is calculated for each interaction strength using eq 7, and the results are shown in Figure 5. We see that c seems to be asymptotically converging to a number somewhat over 6, corresponding approximately to stick boundary conditions.

The fact that the boundary condition coefficient attains values in excess of 6 can be attributed to a number of factors. In our previous work[4] we estimated that finite-size effects for a particle of $M/m = 125$ suppress the diffusion constant (and thus increase the boundary condition coefficient) by 3%. However, in the present context the total mass of our effectively rough sphere is almost $M = 200m$ (including the mass of the permanently affixed solvation shell). Thus, such finite-size effects could cause a more significant increase in the calculated boundary condition coefficient. There is also, as always, some ambiguity in the

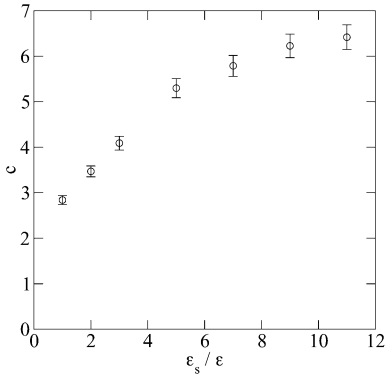

Figure 5. Hydrodynamic boundary condition coefficient values, for the case of short-range isotropic variably attractive solute−solvent interactions, as a function of ϵ_s/ϵ. Note that, as discussed in the text, the effective hydrodynamic radius of the solute is take to be $a + (1 + 2^{1/6})\sigma$.

choice of the appropriate hydrodynamic radius. Finally, although the solvent particles in the solute's first solvation shell are more or less fixed radially, the composite solute (bare solute with its first solvation shell) is still not rigid, and it is possible that low-frequency sloshing modes of the solvation shell serve to decrease the diffusion constant (relative to that of a rigid rough solute of the same mass) and therefore increase the boundary condition coefficient.

To understand when ϵ_s/ϵ is large enough to produce the effectively rough solute, we consider the ratio of the residence time of a solvent particle in the first solvation shell, to the other relevant time scale, which is the hydrodynamic time[7,14]

$$t_h = \rho_m R^2/\eta \tag{11}$$

where ρ_m is the mass density of the bulk solvent. t_h corresponds to the time for a viscous shear wave to propagate across the Brownian particle. The residence time, t_r, can be estimated crudely using transition state theory,

$$\frac{1}{t_r} = \frac{\omega}{2\pi} e^{-E/kT} \tag{12}$$

where ω is the oscillation frequency for the radial motion of a solvent particle in the first solvation shell, and E is the effective energy barrier for escape from the first solvation shell. Both of these quantities can be estimated from the solute−solvent potential of mean force, $w(r) = -kT \ln g(r)$. When $t_r/t_h \gg 1$, the solute and its first solvation shell should act as a composite particle. We find, for example, that $t_r/t_h \approx 27$ when $\epsilon_s/\epsilon = 7$, which indicates that for ϵ_s/ϵ greater than 7 or so, this should be the case. This is consistent with Figure 5, which shows that the stick boundary condition is more or less achieved when ϵ_s/ϵ is on this order.

V. Conclusion

Several model problems were examined to attempt to understand the microscopic origins of the stick boundary condition for the Brownian motion problem. We show that for a solute interacting with solvent particles with a purely repulsive isotropic potential, and also for a weakly attractive isotropic potential (see also ref 4), the Stokes−Einstein equation holds with slip boundary conditions. However, for a rough solute we demonstrate that the Stokes−Einstein equation holds with stick boundary conditions. In both of these cases, the solute radius is taken not to be the bare radius, but the effective hydrodynamic radius. We also show how the rough solute result can be approached continuously by considering a short-range isotropic solute−solvent potential as the attraction increases. When the attraction becomes strong enough so the residence time of the solvation shell particles is long compared to the characteristic hydrodynamic time, the composite solute (bare solute plus first solvation shell) is rough, and so stick boundary conditions apply.

These results verify that on the molecular level it is the surface roughness of the solute that leads to stick boundary conditions. The surface roughness presents a mechanism for the enforcement of the equality of the tangential components of the solute and fluid velocities, leading to stick boundary conditions. Such a mechanism is of course absent for smooth solutes, when slip boundary conditions are more appropriate.

Acknowledgment. J.L.S. is delighted to dedicate this paper to Hans C. Andersen, who has been a mentor and friend for nearly twenty-five years. We are grateful for support from the National Science Foundation, through grant no. CHE-0132538, and from the Fannie and John Hertz Foundation through a fellowship to J.R.S.

References and Notes

(1) Hansen, J.-P.; McDonald, I. R. *Theory of Simple Liquids*, 2nd ed.; Academic: London 1986.
(2) Balucani, U.; Zoppi, M. *Dynamics of the Liquid State*; Clarendon: Oxford, U.K., 1994.
(3) Hynes, J. T. *Annu. Rev. Phys. Chem.* **1977**, *28*, 301.
(4) Schmidt, J. R.; Skinner, J. L. *J. Chem. Phys.* **2003**, *119*, 8062.
(5) Ould-Kaddour, F.; Levesque, D. *Phys. Rev. E* **2000**, *63*, 011205.
(6) Dahneke, B. *Measurement of Suspended Particles by Quasi-Elastic Light Scattering*; John Wiley and Sons: New York, 1983.
(7) Paul, G. L.; Pusey, P. N. *J. Phys. A: Math. Gen.* **1981**, *14*, 3301.
(8) Richardson, S. *J. Fluid Mech.* **1973**, *59*, 707.
(9) Khare, R.; de Pablo, J.; Yethiraj, A. *J. Chem. Phys.* **1997**, *107*, 2589.
(10) Koplik, J.; Banavar, J. R.; Willemsen, J. F. *Phys. Fluids A* **1989**, *1*, 781.
(11) Bocquet, L.; Barrat, J. *Phys. Rev. Lett.* **1993**, *70*, 2726.
(12) Thompson, P. A.; Robbins, M. O. *Phys. Rev. A* **1990**, *41*, 6830.
(13) Vergeles, M.; Keblinkski, P.; Koplik, J.; Banavar, J. R. *Phys. Rev. E* **1996**, *53*, 4852.
(14) Heyes, D. M.; Nuevo, M. J.; Morales, J. J.; Branka, A. C. *J. Phys.: Condens. Matter* **1998**, *10*, 10159.
(15) Masters, A. J.; Madden, P. A. *J. Chem. Phys.* **1981**, *74*, 2450.
(16) Biswas, R.; Bhattacharyya, S.; Bagchi, B. *J. Phys. Chem. B* **1998**, *102*, 3252.
(17) Srinivas, G.; Bhattacharyya, S.; Bagchi, B. *J. Chem. Phys.* **1999**, *110*, 4477.
(18) Zwanzig, R.; Bixon, M. *Phys. Rev. A* **1970**, *2*, 2005.
(19) Keyes, T.; Oppenheim, I. *Phys. Rev. A* **1973**, *8*, 937.
(20) Peralta-Fabi, R.; Zwanzig, R. J. *Chem. Phys.* **1979**, *70*, 504.
(21) Zwanzig, R.; Harrison, A. K. J. *Chem. Phys.* **1985**, *83*, 5861.
(22) Bhattacharyya, S.; Bagchi, B. J. *Chem. Phys.* **1997**, *106*, 1757.
(23) Murarka, R.; Bhattacharyya, S.; Bagchi, B. *J. Chem. Phys.* **2002**, *117*, 10730.
(24) Dekker, H. *Physica A* **1983**, *117*, 1.
(25) van Beijeren, H.; Dorfman, J. R. *J. Stat. Phys.* **1980**, *23*, 335.
(26) Weeks, J. D.; Chandler, D.; Andersen, H. C. *J. Chem. Phys.* **1971**, *54*, 5237.
(27) Rull, L. F.; de Miguel, E.; Morales, J. J.; Nuevo, M. J. *Phys. Rev. A* **1989**, *40*, 5856.
(28) Laird, B. B.; Skinner, J. L. *J. Chem. Phys.* **1989**, *90*, 3274.
(29) Allen, M. P.; Tildesley, D. J. *Computer Simulation of Liquids*; Clarendon: Oxford, U.K., 1987.
(30) Steinbach, P. J.; Brooks, B. R. *J. Comput. Chem.* **1994**, *15*, 667.